

Benchmark test: Description of prompt-neutron spectra with the GEF code ^{*}

Karl-Heinz Schmidt[†]
Beatriz Jurado[‡]

January 2014

1 Introduction

This work deals with the description of prompt-neutron spectra in neutron-induced fission reactions over a larger excitation-energy range extending from spontaneous fission to multi-chance fission. A number of measured prompt-neutron spectra from elaborate experiments are compared with the results of the GEF code [1, 2]. The GEF code calculates the contributions from the excited nucleus before scission and from the fragments simultaneously with the statistical model in a consistent way together with many other fission observables. The calculation is done without using an analytical formula with adjustable parameters for the shape of the prompt-neutron spectrum and without any input on fission-fragment properties for specific systems. Therefore, this study is aimed to give a coherent picture on the variation of the prompt-neutron spectrum for different fissioning systems as a function of excitation energy.

^{*}Contribution to the IAEA Coordinated Research Program on Prompt Fission Neutron Emission, January 2014

[†]E-mail: schmidt-erzhausen@t-online.de, URL: <http://www.khs-erzhausen.de>

[‡]E-mail: jurado@cenbg.in2p3.fr, CENBG, CNRS/IN2 P3, Chemin du Solarium B.P. 120, F-33175 Gradignan, France

2 Description of the calculation

The following figures show comparisons of measured fission prompt-neutron spectra extracted from EXFOR with results of the GEF code [1, 2]. All measurements have been performed relative to the system $^{252}\text{Cf}(\text{sf})$. Thus, the data marked as ratio or R are directly measured. If the deduced prompt-neutron spectra are also given in EXFOR, they are shown as well, marked as yield or Y. The scale is dN/dE in units of $1/\text{MeV}$.

GEF calculations on neutron yields and energy distributions have been performed for the indicated systems and for $^{252}\text{Cf}(\text{sf})$. All calculations have been performed without any adjustment to specific systems with the very same parameter set. No particular information from experimental data, e.g. *A*-TKE spectra, has been used. The GEF model exploits three general laws of dynamics, quantum mechanics and statistical mechanics in order to model the fission process in a comprehensive and consistent way with a modest input of empirical information and a minimum of computational effort: The influence of inertia and friction on the fission dynamics is implicitly considered by a dynamical freeze-out, the influence of nuclear structure is traced back to the early influence of fragment shells, and the transport of thermal energy between the fragments before scission is assumed to be driven by entropy.

In order to clearly distinguish the general approach of the GEF model from other models, a short summary of alternative approaches seems to be appropriate. One of the first widespread description of the prompt-neutron spectrum was introduced by Watt [3]. He proposed a closed formula, deduced from a Maxwell-type energy spectrum from one or two average fragments and the transformation into the frame of the fissioning system with at least two adjustable parameters: the temperature and the velocity of the average fragment. The "Los-Alamos model" [4] extended this approach essentially by the use of a triangular temperature distribution of the fragments to a four-term closed expression for an average light and an average heavy fragment. A similar two-fragment model was also used by Kornilov et al. in ref. [5]. In 1989, Madland et al. [6] introduced the point-by-point model by considering the emission from all individual fragments, specified by *Z* and *A*. This model was further developed e.g. by Lemaire et al. [7], Tudora et al. [8] and Vogt et al. [9]. In refs. [10, 11, 12, 13], the spectral shape was parameterised by the Watt formula [3] or an empirical shape function that had been introduced by Mannhart [14] in order to better model the shape of the neutron energy spectra in the fragment frame. Kornilov [15] proposed a phenomenological approach for the parameterisation of a model-independent

shape of the prompt-neutron spectrum. This approach was later also used by Kodeli et al. [16] and Maslov et al. [17]. These models often reach a high degree of agreement with the measured prompt-neutron spectra for particular fissioning systems with especially adjusted parameters. All models cited above are based on empirical data: The Watt model and the Lost-Alamos model are directly fitted to the measured prompt-neutron spectrum, while the point-by-point model is based on the measured A -TKE distribution. Manea et al. [18] proposed a scission-point model that predicts the TKE(A) distribution, in order to allow for calculations of prompt-neutron spectra with the point-by-point method if only the mass distribution is known. For completeness we also mention a paper of Howerton [19], who developed a method for predicting (Z, A, E_n) distributions. The required input values are the charge and mass numbers (Z and A) and the binding energy of the last neutron in the $(A + 1)$ nucleus. Unfortunately, we did not yet have access to this paper. This method was used in ref. [20].

As a result of the GEF model, the prompt-neutron spectra and the ratios to the calculated $^{252}\text{Cf}(\text{sf})$ spectrum are shown. Due to the Monte-Carlo method used in the GEF code, the spectra show statistical fluctuations, especially in the high-energy tail. The calculated total prompt-neutron multiplicity is given in addition in the figures. Note that the deviations between GEF results and experimental data in the two representations (ratio and yield) are not consistent, because the GEF yield ratios and the experimental yields (measured yield ratios times neutron yields for $^{252}\text{Cf}(\text{sf})$) have been obtained with different prompt-neutron reference spectra: For the GEF ratios the calculated $^{252}\text{Cf}(\text{sf})$ spectrum was used, for the experimental yields an evaluated $^{252}\text{Cf}(\text{sf})$ spectrum was used. It seems that most of the experiments aimed only to determine the shape of the spectra. Therefore, an arbitrary scaling factor was applied, such that the total prompt-neutron multiplicity agrees approximately with the GEF result. These scaling factors are listed in the legends of the figures. All figures are shown in logarithmic and in linear scale.

3 Results

3.1 Spectra

$^{232}\text{Th}(\text{n,f})$, $E_n=2.9$ MeV: The calculated spectrum is slightly softer than the measured one.

$^{232}\text{Th}(\text{n,f})$, $E_n=14.7$ MeV: Most part of the spectrum is very well reproduced by the calculation. However, there is a local enhancement at

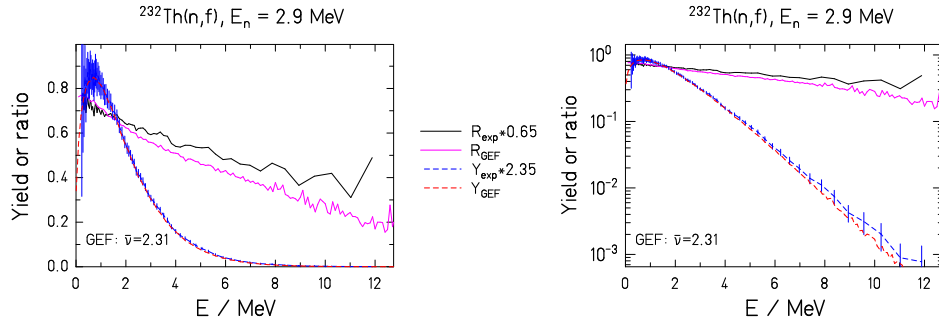


Figure 1: Data from EXFOR dataset 411100081

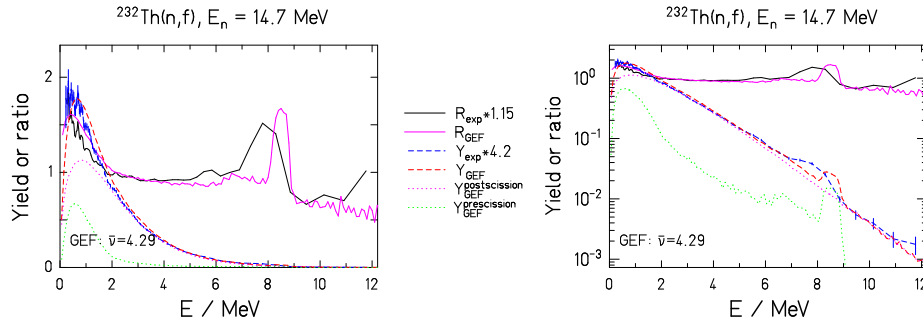


Figure 2: Data from EXFOR dataset 411100081

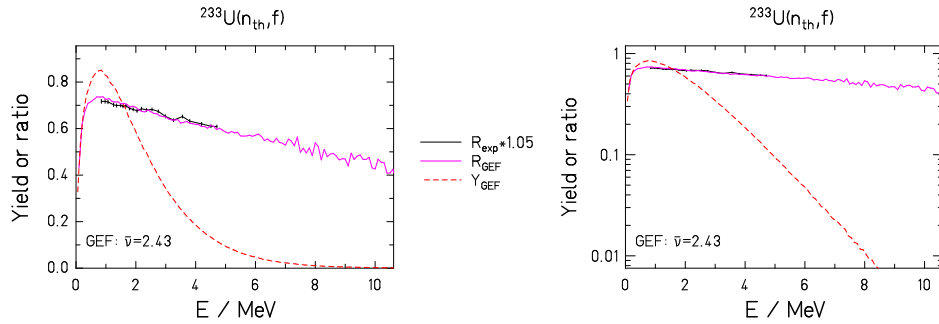


Figure 3: Data from EXFOR dataset 40871013

very low energies, which is not present in the calculation. There seems to be a source for neutrons below 1 MeV in the reference frame of the fissioning system that is not accounted for in the model. The structure around 8 MeV

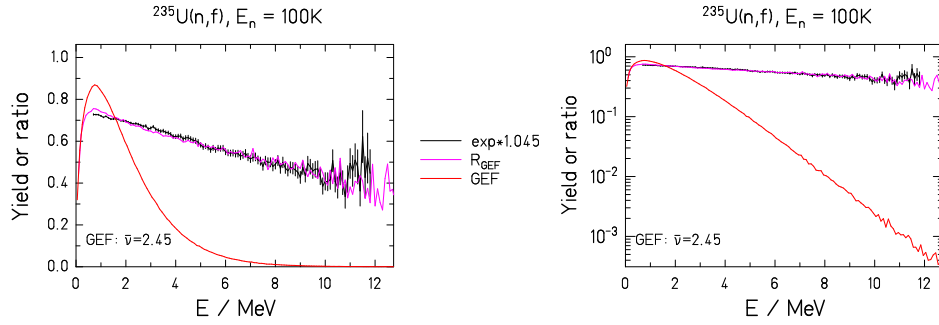


Figure 4: Data from EXFOR dataset 31692006

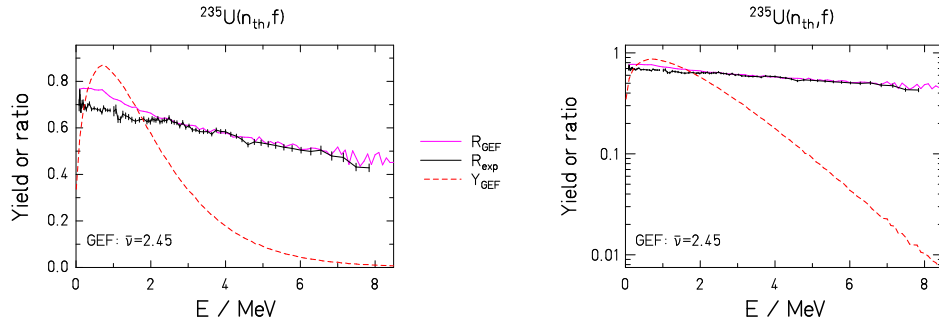


Figure 5: Data from EXFOR datasets 40871011, 40871012

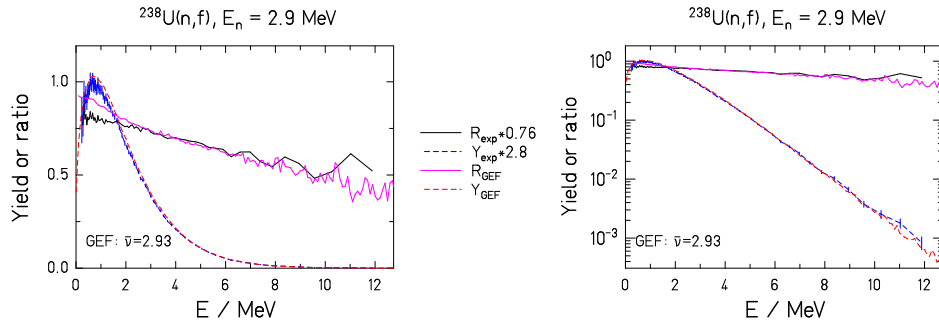


Figure 6: Data from EXFOR dataset 411100101

is narrower and slightly shifted in the calculation.

$^{233}\text{U}(\mathbf{n}_{th}, \mathbf{f})$: The calculated spectrum is very well reproduced in the range between 0.8 and 4.7 MeV that is covered by the experiment.

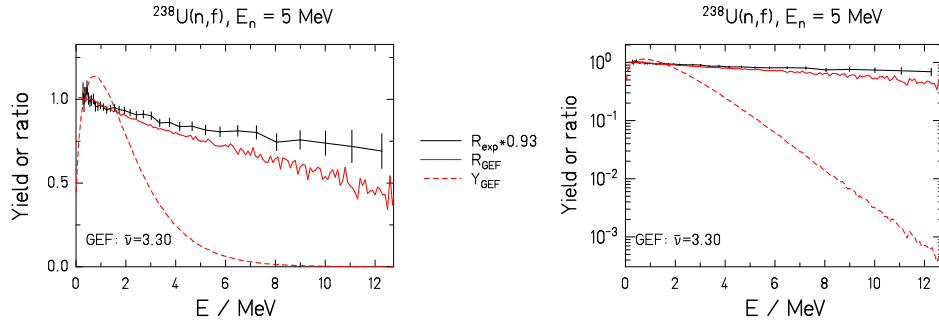


Figure 7: Data from EXFOR dataset 41450003

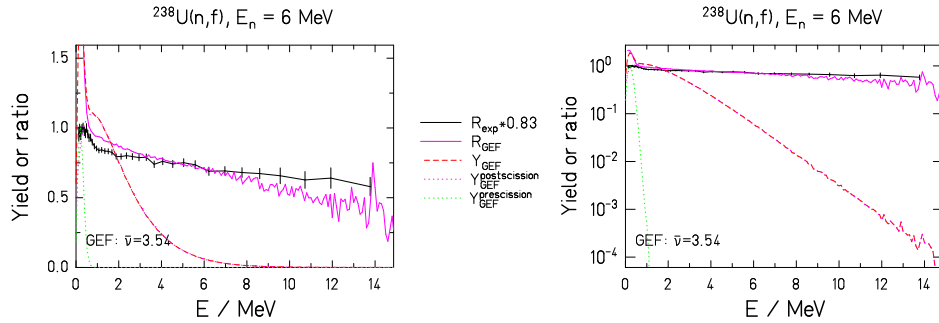


Figure 8: Data from EXFOR dataset 41447003

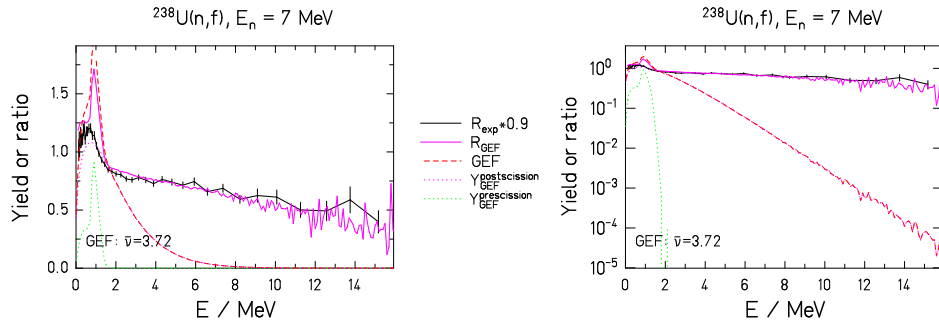


Figure 9: Data from EXFOR dataset 41447003

$^{235}\text{U}(\text{n},\text{f}), E_n=100 \text{ K}$: The spectrum is very well reproduced over almost the whole energy range. Only below 1.5 MeV, the calculated spectrum is a little bit higher. This is in contrast to the comparison of the

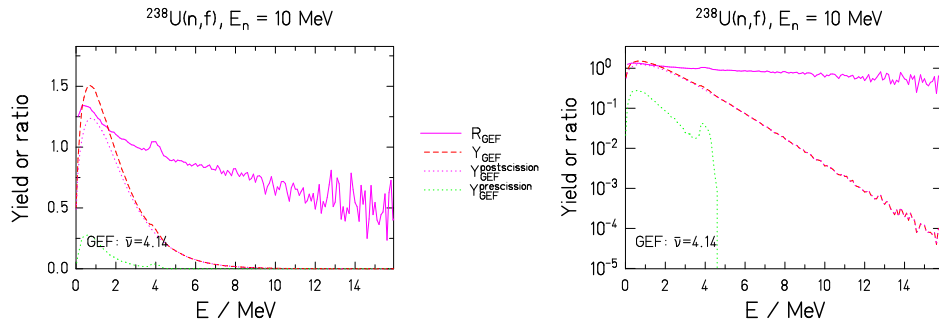


Figure 10: No data available

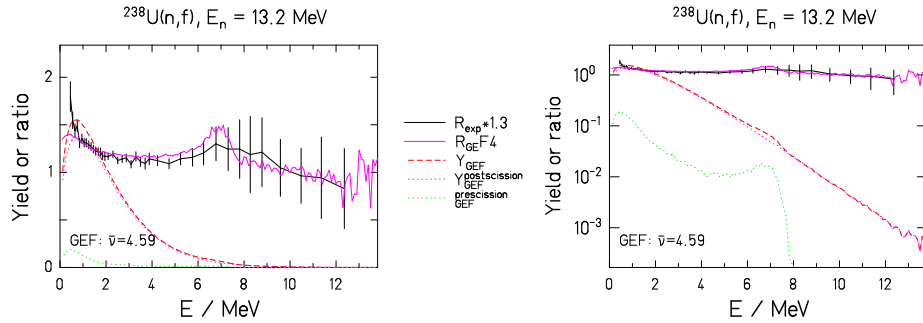


Figure 11: Data from EXFOR dataset 41450003

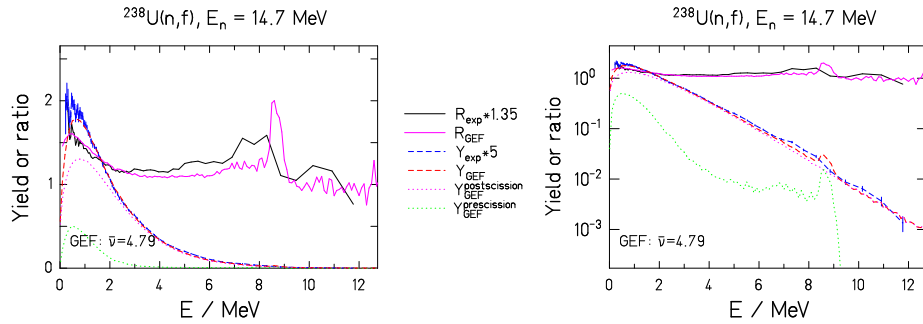


Figure 12: Data from EXFOR dataset 411100101

model calculation with the spectrum in figure 10 of the report from October 2013 of the same authors. Those data were taken from <https://www-nds.iaea.org/pfns/expdata/Kornilov/U235-Kornilov.txt> (uploaded by N. Ko-

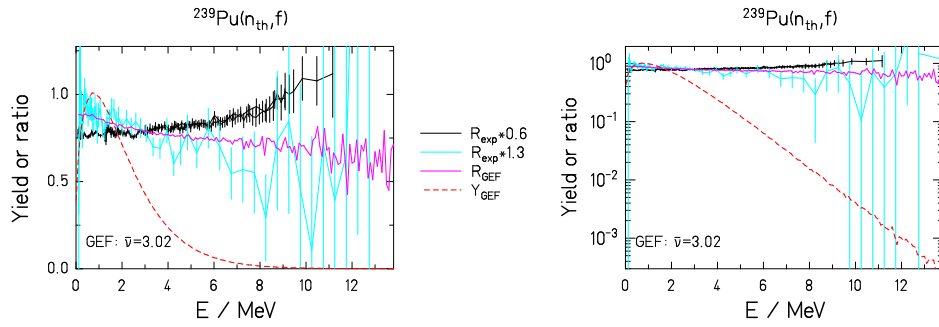


Figure 13: Data from EXFOR datasets 40871009, 40871010, 40872006, 41502004

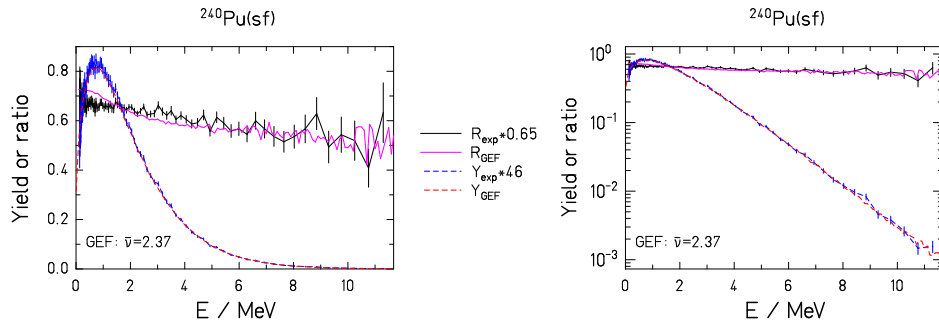


Figure 14: Data from EXFOR dataset 414210021

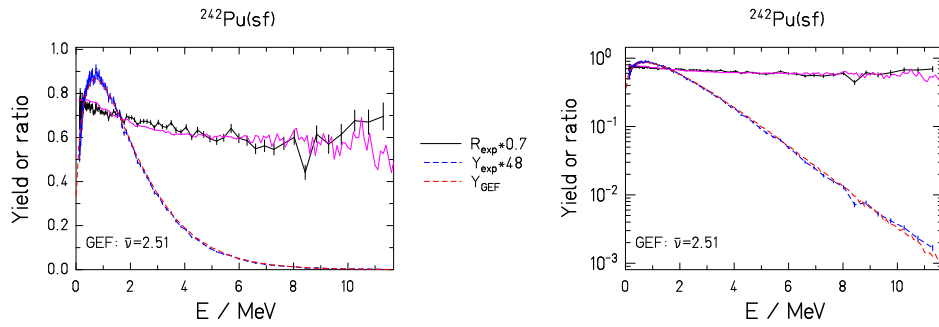


Figure 15: Data from EXFOR dataset 414210031

rnilov 11. Jan. 2011 to <https://www-nds.iaea.org/pfns/>, the working space for participants in the IAEA CRP on "Prompt Fission Neutron Spectra of

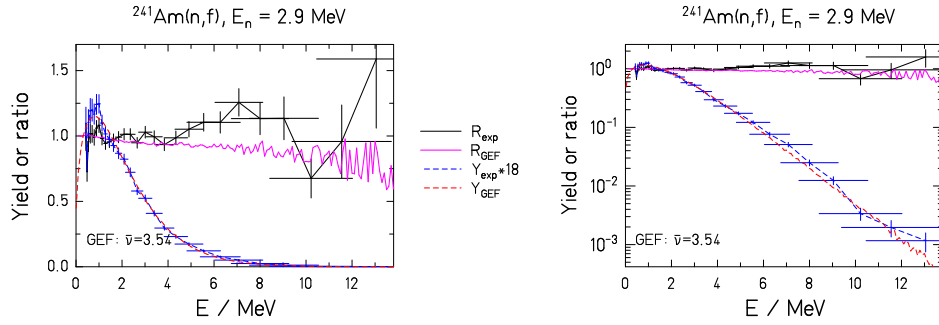


Figure 16: Data from EXFOR dataset 415890021

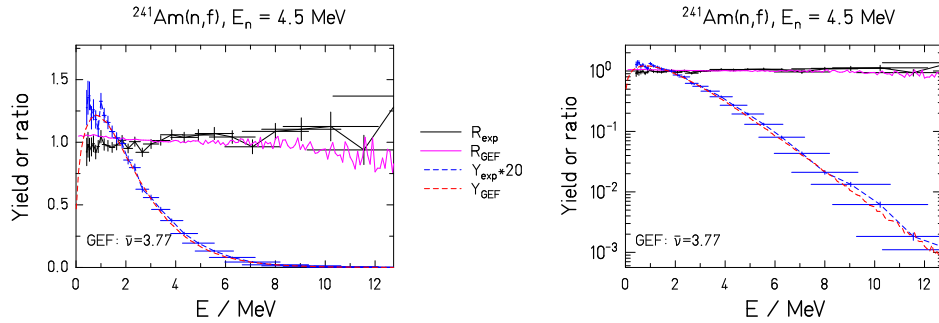


Figure 17: Data from EXFOR dataset 415890031

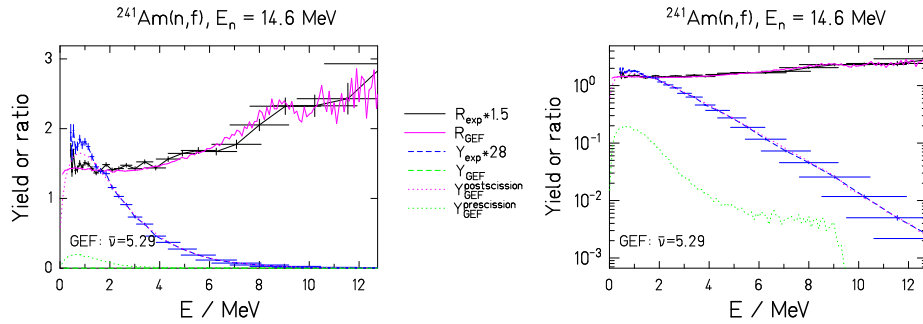


Figure 18: Data from EXFOR dataset 415890041

Actinides”.

$^{235}\text{U}(\mathbf{n}_{th}, \mathbf{f})$: The calculated spectrum shows slight deviations from the measured data. In particular, the calculated spectrum is higher at low

energies below 2 MeV.

$^{238}\text{U}(\mathbf{n},\mathbf{f})$, $E_n=2.9$ MeV: The measured spectrum is well reproduced in the energy range above 2.9 MeV. There is an increasingly enhanced calculated yield towards lower energies.

$^{238}\text{U}(\mathbf{n},\mathbf{f})$, $E_n=5$ MeV: The slope of the calculated spectrum is steeper than the one of the measured spectrum. At 12 MeV, the calculated spectrum is about 40 % lower than the measured one.

$^{238}\text{U}(\mathbf{n},\mathbf{f})$, $E_n=6$ MeV: The comment for the preceding case is also valid here. In addition, the spectrum is enhanced at the lowest energies due to a contribution from second-chance fission. This enhancement is overestimated by the calculation. The amplitude of the structure below 1 MeV is overestimated and too narrow.

$^{238}\text{U}(\mathbf{n},\mathbf{f})$, $E_n=7$ MeV: The slope of the spectrum is only slightly overestimated by the model. The spectrum is enhanced at the lowest energies due to a contribution from second-chance fission. Amplitude, width and position of this structure are not correctly reproduced by the calculation.

$^{238}\text{U}(\mathbf{n},\mathbf{f})$, $E_n=10$ MeV: This spectrum, for which no data are available, is added in order to allow a systematic view on the variation of the structure caused by the threshold of second-chance fission.

$^{238}\text{U}(\mathbf{n},\mathbf{f})$, $E_n=13.2$ MeV: The spectrum is well reproduced by the model within the experimental uncertainties. However, there is a local enhancement at very low energies, which is not present in the calculation. There seems to be a source for neutrons below 1 MeV in the reference frame of the fissioning system that is not accounted for in the model, like in the case of $^{232}\text{Th}(\mathbf{n},\mathbf{f})$ at $E_n=4.7$ MeV. The structure due to the threshold of second-chance fission is slightly shifted to lower energies and narrower in the calculation.

$^{238}\text{U}(\mathbf{n},\mathbf{f})$, $E_n=14.7$ MeV: Again, there is a local enhancement at very low energies below 0.6 MeV, which is not strong enough in the calculation. The shape and the position of the structure due to the threshold of second-chance fission are not correctly reproduced by the calculation.

$^{239}\text{Pu}(\mathbf{n}_{th},\mathbf{f})$: There are two experimental results with different slopes of the high-energy tail. The slope of the calculated spectrum agrees better with the steeper slope of one of the experiments, although this spectrum shows strong local fluctuations. The steeper slope is also much closer to the ones of the systems $^{238}\text{U}(\mathbf{n},\mathbf{f})$, $E_n=2.9$ MeV and $^{246}\text{Cm}(\text{sf})$, which have similar total prompt-neutron yields as $^{239}\text{Pu}(\mathbf{n}_{th},\mathbf{f})$. Since all these cases are restricted to first-chance fission, one should expect that the total prompt-neutron yield is a measure of the mean excitation energies of the primary fragments, which means that it should be correlated with the slope of the

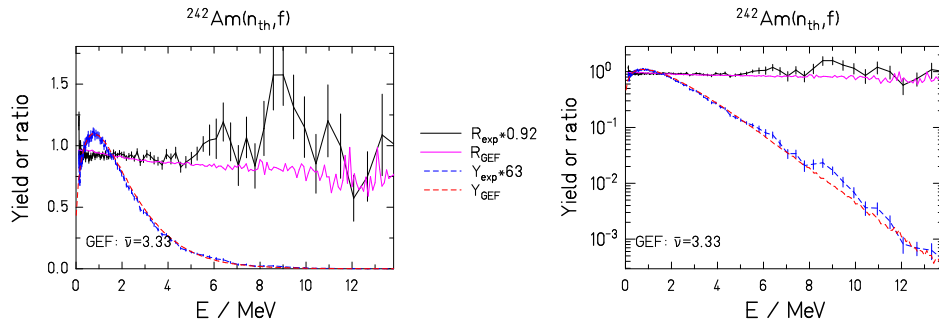


Figure 19: Data from EXFOR dataset 414210081

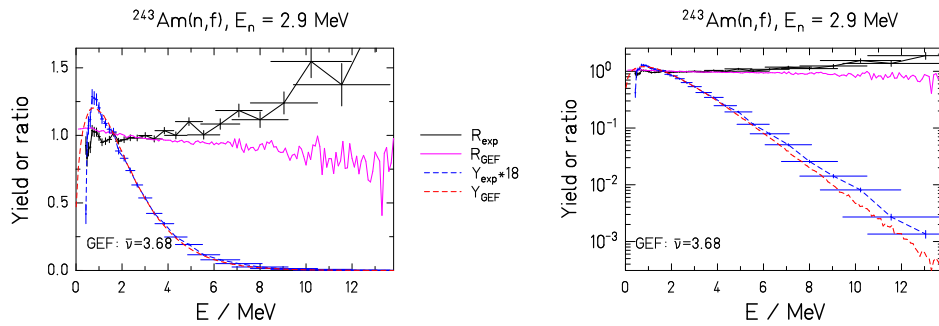


Figure 20: Data from EXFOR dataset 415890051

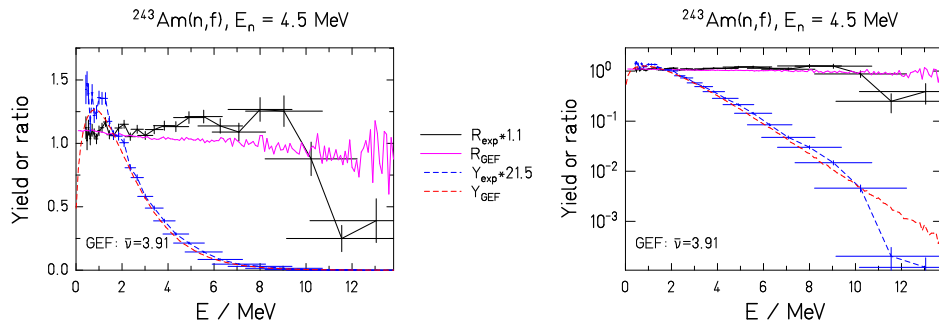


Figure 21: Data from EXFOR dataset 415890061

high-energy tail of the prompt-neutron spectrum. Due to this argument, the spectrum with the steeper slope appears to be more likely the correct one.

$^{240}\text{Pu}(\text{sf})$, $^{242}\text{Pu}(\text{sf})$: The measured spectra are well reproduced by

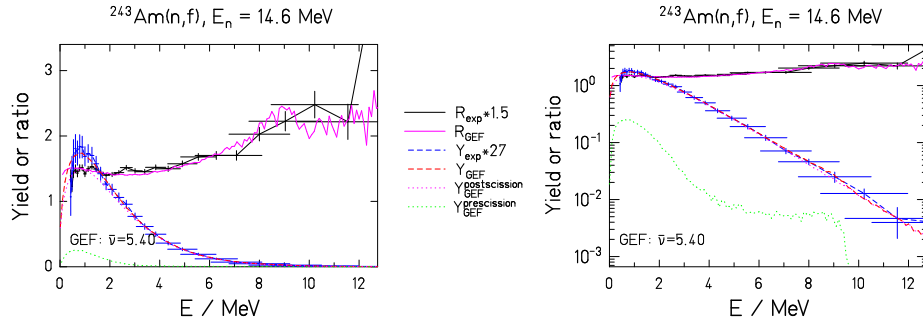


Figure 22: Data from EXFOR dataset 415890071

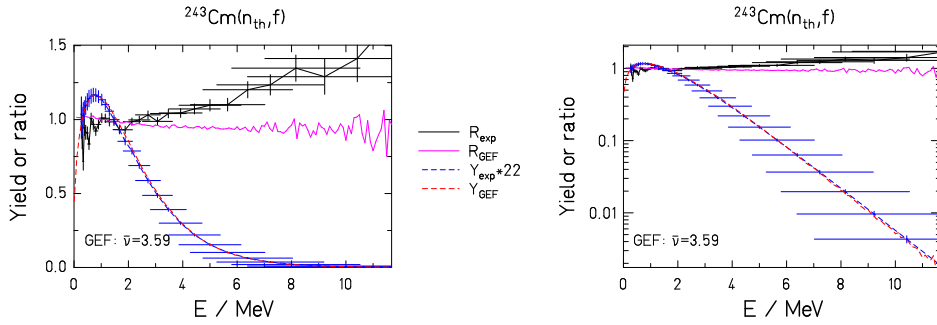


Figure 23: Data from EXFOR dataset 415890081

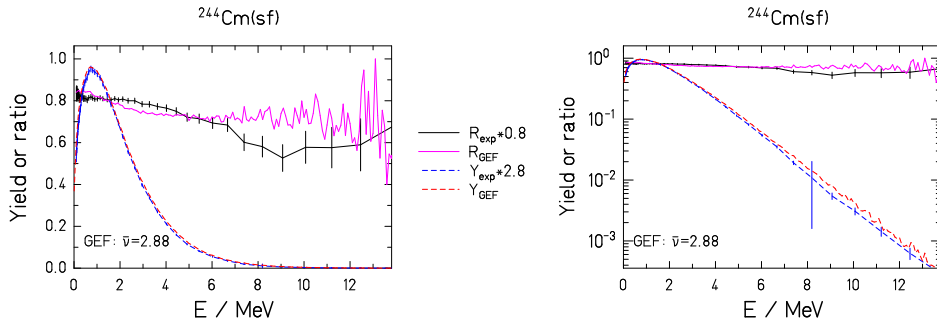


Figure 24: Data from EXFOR dataset 413400041

the calculation.

$^{241}\text{Am}(\text{n},\text{f})$, $E_n=2.9$ MeV: Below 4 MeV, the measured spectrum is well reproduced by the calculation. A comparison at higher energies is

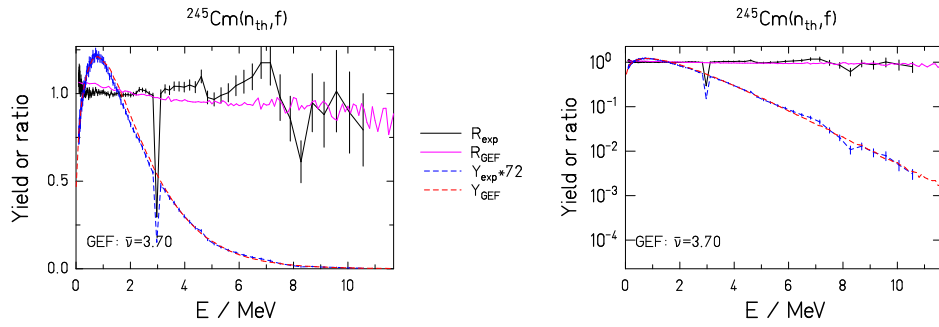


Figure 25: Data from EXFOR dataset 414210091

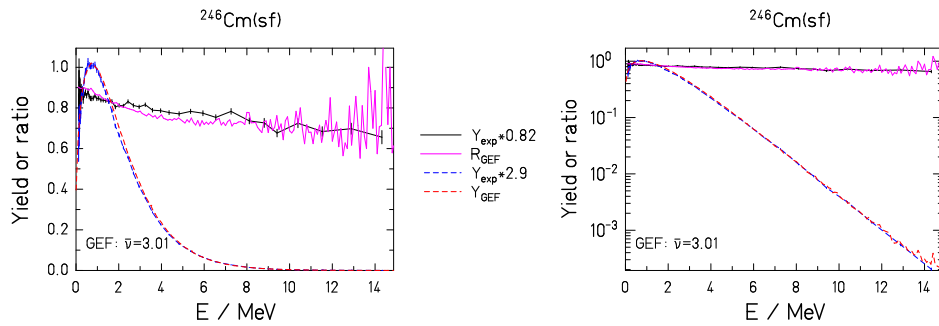


Figure 26: Data from EXFOR dataset 413400051

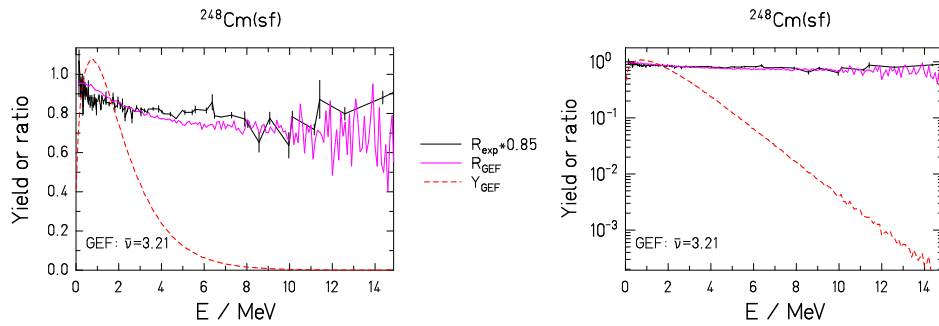


Figure 27: Data from EXFOR dataset 41113004

difficult due to the strong fluctuations in the measured spectrum.

$^{241}\text{Am}(n,f)$, $E_n=4.5$ MeV: The measured spectrum is well reproduced by the calculation. There are slight deviations above 8 MeV, but the exper-

imental data fluctuate here rather strongly.

²⁴¹**Am(n,f), $E_n=14.6$ MeV:** The measured spectrum is well reproduced by the calculation, including the structure around 9 MeV.

²⁴²**Am(n_{th},f):** Below 5 MeV, the measured spectrum is well reproduced by the calculation. A comparison is difficult at higher energies due to the strong fluctuations in the measured spectrum.

²⁴³**Am(n,f), $E_n=2.9$ MeV:** The calculated spectrum is much softer in the high-energy tail than the measured one. It is remarkable that the measured spectrum is appreciably stiffer than the spectrum of ²⁵²Cf(sf), although the total prompt neutron yield is almost the same.

²⁴³**Am(n,f), $E_n=4.5$ MeV:** In the energy range below 8 MeV, the calculated spectrum is slightly softer than the measured one. A comparison at higher energies is difficult due to the strong fluctuations of the measured spectrum.

²⁴³**Am(n,f), $E_n=14.6$ MeV:** The measured spectrum is generally well reproduced by the calculation. The structure around 8 MeV is slightly shifted to lower energies.

²⁴³**Cm(n_{th},f):** When comparing the measured and the calculated ratios to the spectrum of ²⁵²Cf(sf), the calculated spectrum appears to be much softer than the measured one. It is astonishing that the measured spectrum is as stiff as the one for ²⁴³Am(n,f) at $E_n=14.6$ MeV which has a much higher total prompt-neutron yield. The measured spectrum is also much stiffer than the one of the system ²⁵²Cf(sf), although the total prompt-neutron yield is about the same. However, when comparing the empirical prompt-neutron spectrum, already multiplied with the reference spectrum of ²⁵²Cf(sf), which is also listed in EXFOR, with the calculated spectrum, in particular in logarithmic scale in the left panel, there is very good agreement. This kind of inconsistency is not observed for any other case.

²⁴⁴**Cm(sf):** The measured spectrum has an unusual shape with a dip around 9 MeV. This dip is not found in the calculated spectrum.

²⁴⁵**Cm(n_{th},f):** In the range below 4.6 MeV, the calculated spectrum is slightly softer than the measured one. (One value at 3 MeV seems to be in error.) At higher energies, the measured spectrum shows strong fluctuations.

²⁴⁶**Cm(sf) and ²⁴⁸Cm(sf):** Both measured spectra are well reproduced by the calculation within the experimental uncertainties.

4 Discussion

4.1 General observations

The most salient features of this comparison are:

1. There is a qualitatively rather good reproduction of the shape of the spectra, including the structural effects. There are some deviations in the quantitative reproduction of the structure at the threshold of second-chance fission.
2. In some cases, the exponential slope of the calculated spectrum exceeds the slope of the measured spectrum. The most important deviations are found for $^{238}\text{U}(\text{n},\text{f})$, $E_n=5$ and 6 MeV, $^{239}\text{Pu}(\text{n}_{th},\text{f})$ with respect to one experiment, $^{243}\text{Am}(\text{n},\text{f})$, $E_n=2.9$ MeV, and $^{243}\text{Cm}(\text{n}_{th},\text{f})$.
3. There are some fluctuations in the data for which the model does not provide an explanation. The most severe cases are $^{241}\text{Am}(\text{n},\text{f})$, $E_n=2.9$ MeV, $^{242}\text{Am}(\text{n}_{th},\text{f})$, ^{243}Am , $E_n=4.5$ MeV, and $^{243}\text{Cm}(\text{n}_{th},\text{f})$.
4. Two experiments for $^{239}\text{Pu}(\text{n}_{th},\text{f})$ give diverging results.
5. There are some inconsistencies in different data tables from the same experiment, e.g. for $^{243}\text{Cm}(\text{n}_{th},\text{f})$ and $^{235}\text{U}(\text{n}_{th},\text{f})$. In both cases, there is very good agreement of the calculated prompt-neutron spectrum with one set of data, while another dataset deviates.

4.2 Pre-fission neutron emission

The pre-fission neutrons are registered in coincidence with fission only if the excitation energy of the residual nucleus falls above its fission barrier. This causes a pronounced structure in the prompt-fission-neutron spectrum. The structure of the calculated spectrum reproduces the structure in the measured spectra rather well in most cases. In the calculations, the structure depends on the description of pre-scission neutron emission, pre-equilibrium and statistical, as well as on the excitation-energy-dependent fission probabilities of the different nuclei. In particular, the mean energy of the structure in the calculated spectra depends on the value of the fission threshold in the GEF code. In particular for even-even fissioning nuclei, the number and the nature of levels at the fission barrier below the pairing gap are subject to strong nuclear-structure effects [21] and difficult to model with a global approach. In the experiment, the width of this structure is very sensitive to

the energy spread of the incoming neutrons and the energy resolution in the measurement of the emitted neutrons. The mean energy is very sensitive to the energy definition of the incoming neutrons.

4.3 Inverse cross section

Since the evaporation spectrum is calculated with a modified Weisskopf formalism where the angular momentum is explicitly considered, the mass- and energy-dependent transmission coefficients for neutron emission were parameterised by using inverse capture cross sections according to Dostrowsky et al. [22] in a slightly modified version for fast computing.¹

Since the fast-neutron spectrum in fission is composed of the contributions from many emitting fragments, the use of this global description is probably not too critical.

5 Conclusion

The model behind the GEF code is unique in the sense that it provides practically all observables from nuclear fission without any needs for specific experimental information by using a single fully consistent model description for all heavy fissioning systems. The present comparison with measured prompt-neutron spectra shows good agreement in most cases, but also some deviations, mostly in the high-energy tail of the spectrum and in the structures caused by threshold effects in pre-fission neutron emission. These structures are not exactly reproduced by the calculation, although their integral strength and their position in energy deviate only little. In particular in the fission of the lighter systems at higher energies, the model does not provide enough intensity at low energies, mostly below 1 MeV, in the frame of the fissioning system. Some of this additional intensity is explained by the emission during the acceleration phase, but this contribution does not reach far enough down in energy. There seems to be a source of very low-energetic neutrons with an exponential-like spectrum in the frame of the fissioning system, which is not accounted for in the model. This problem has already been discussed in refs. [20, 10]. A possible origin of these low-energy neutrons could be the pre-acceleration emission from fragments with very large

¹The present version of the GEF code is conceived as a very fast code. Whenever possible, fast algorithms were used as long as their approximations do not exceed the estimated general uncertainties of the model. They may easily be replaced by more elaborate descriptions in the freely accessible code.

transmission coefficients at low energies, which are not accounted for in the global description used in the present model.

A systematic view on the experimental data suggests that the uncertainties are underestimated in several cases. There are strange fluctuations in the measured spectra for $^{241}\text{Am}(\text{n},\text{f})$, $E_n=2.9$ MeV, for $^{242}\text{Am}(\text{n}_{\text{th}},\text{f})$, for $^{243}\text{Am}(\text{n},\text{f})$, $E_n=4.5$ MeV, and for $^{245}\text{Cm}(\text{n}_{\text{th}},\text{f})$. Contradictory results were obtained from different experiments for $^{239}\text{Pu}(\text{n}_{\text{th}},\text{f})$. In the energy range up to $E_n = 7$ MeV, where at least most part of the spectrum is only fed by first-chance fission, the high-energy tail of the measured spectra becomes in general stiffer with increasing energy of the impinging neutron. This trend is weaker in the calculated spectra in some cases. But the variation of the stiffness is not continuous in the data as a function of the incoming-neutron energy. Sometimes, e.g. for $^{238}\text{U}(\text{n},\text{f})$ at $E_n = 7$ MeV, the spectrum becomes softer again with increasing energy of the incoming neutrons. Moreover, the variations from one system to another one are not consistent with the model. After a careful analysis of this problem, the situation appears to be unclear. On the one hand, the mean temperature of the emitting fragments is expected to increase with increasing incoming-neutron energy. Thus, the trend to stiffer prompt-neutron spectra found in the experiment is qualitatively expected. On the other hand, these experiments are certainly very challenging, and some results may suffer from an incompletely suppressed background of scattered neutrons. This might be the reason for some unexpected fluctuations of the logarithmic slope of the spectra from one system to another as a function of incoming-neutron energy or total prompt-neutron yield. More data of high quality would certainly be helpful for a better understanding of this problem.

One may conclude that it is the merit of the GEF model to provide a global view on the systematic variation of the fission observables as a function of the fissioning system and its excitation energy. It reproduces the measured prompt-neutron spectra in general rather well. A detailed analysis reveals three types of deviations that are found for some of the systems: The description of the structure in the prompt-neutron spectrum due to the contribution of second-chance fission suffers probably from difficulties in modeling the level densities of even-even nuclei below the pairing gap by the global approach used in the code. Furthermore, there seems to be a source for the emission of neutrons with very low energies in some systems before or slightly after fission that is not sufficiently accounted for in the model. Finally, we think that there are indications that the stiffness of the prompt-neutron spectra is distorted in several cases by an incompletely suppressed background of scattered neutrons. Predictions for other systems

where no experimental data are available are expected to be possible with similar quality.

Acknowledgement

This work has been supported by the NEA of the OECD (<http://www.oecd-nea.org/>) and by the EFNUDAT (<http://www.efnudat.eu/>) and by the ERINDA (<http://www.erinda.org/>) projects of the European Union.

References

- [1] K.-H. Schmidt, B. Jurado, JEF/DOC 1423, NEA of OECD, Paris, 2011, available from [2].
- [2] <http://www.cenbg.in2p3.fr/GEF>, <http://www.khs-erzhausen.de>
- [3] B. E. Watt, Phys. Rev. 87 (1952) 103.
- [4] D. Madland, J. Nix, Nucl. Sci. Eng. 81 (1982) 213
- [5] N. V. Kornilov et al., Phys. Atom. Nuclei 64 (2001) 1451.
- [6] Madland, D.G., LaBauve, R.J., Nix, J.R., 1989. IAEA-INDC(NDS)-220, 259.
- [7] S. Lemaire, P. Talou, T. Kawano, M. B. Chadwick, D. G. Madland, Phys. Rev. C 72 (2005) 024601
- [8] A. Tudora, F.-J. Hamsch, Ann. Nucl. Energy 37 (2010) 771.
- [9] R. Vogt, J. Randrup, D. A. Brown, M. A. Descalle, W. E. Ormand, Phys. Rev. C 85 (2012) 024608
- [10] M. I. Svirin, G. N. Lovchikova, A. M. Trufanov, Phys. Atom. Nuclei 60 (1997) 727.
- [11] A. M. Trufanov et al., Phys. Atom. Nuclei 64 (2001) 1.
- [12] G. N. Lovchikova et al., Phys. Atom. Nuclei 67 (2004) 1246.
- [13] V. M. Maslov, At. Energy 103 (2007) 633.
- [14] W. Mannhart, IAEA-TECDOC-410 (IAEA, Vienna, 1987), p. 158.
- [15] M. V. Kornilov et al., Phys. Atom. Nuclei 62 (1999) 209.

- [16] I. Kodeli et al., Nucl. Instrum. Methods A 610 (2009) 540.
- [17] V. M. Maslov et al., J. Korean Phys. Soc. 59 (2011) 1337.
- [18] V. Manea, A. Tudora, Ann. Nucl. Energy 38 (2011) 72.
- [19] R. J. Howerton, Nucl. Science Engineering 62 (1977) 438.
- [20] G. S. Boykov et al., Nucl. Energy 21 (1994) 585.
- [21] B. B. Back, Ole Hansen, H. C. Britt, J. D. Garret, Phys. Rev. C 9 (1974) 1924.
- [22] I. Dostrowsky, Z. Fraenkel, G. Friedlander, Phys. Rev. 116 (1959) 683.